

¹¹D. H. Rank and J. N. Shearer, *J. Opt. Sci. Am.* **46**, 463 (1956).

¹²The fs energy levels were obtained from Ref. 6, p. 77.

¹³E. U. Condon and G. H. Shortley, *The Theory of Atomic Spectra* (Cambridge U.P., London, 1959).

¹⁴L. A. Vainshtein and L. A. Minaeva, *Ah. Priklad. Spektrosk. (USSR)* **8**, 244 (1968).

¹⁵H. Kopfermann, *Nuclear Moments*, (Academic, New York, 1958).

¹⁶G. M. Groszof, P. Buck, W. Lichten, and I. I. Rabi, *Phys. Rev. Letters* **1**, 214 (1958).

¹⁷J. T. Latourrette, W. E. Quinn, and N. F. Ramsey, *Phys. Rev.* **107**, 1202 (1957).

¹⁸W. J. Childs, *Phys. Rev. A* **2**, 316 (1970).

¹⁹Kopfermann (Ref. 15) gives expressions for *sp* and *pp'* magnetic dipole matrix elements and *sp* electric quadrupole matrix elements. The latter formula, first given by Casimir [H. Casimir, *Teylors Tweede Genootshap* **11**, 255 (1936)] is inconsistent with the matrix elements in Ref. 16, and appears to be in error. The "12" in the third term on the right-hand side of Ref. 15, Eq. (31.4), should be a "6." We wish to thank W. J. Childs for his helpful comments and for pointing this out.

²⁰The isotopic mixture of the Ne²¹ sample used was

87.9% Ne²¹; 10.2% Ne²⁰; 1.9% Ne²².

²¹R. M. Sternheimer, *Phys. Rev.* **84**, 244 (1951).

²²R. M. Sternheimer, *Phys. Rev.* **164**, 10 (1967).

²³R. M. Sternheimer and R. F. Peierls, *Phys. Rev. A* **4**, 1722 (1971).

²⁴R. M. Sternheimer (private communication). We are grateful to Dr. Sternheimer for providing us with the results of his calculation.

²⁵H. F. Schaefer, III and R. A. Klemm, *Phys. Rev. A* **1**, 1063 (1970).

²⁶Calculations of the *LS* admixture coefficients based on the fs energy splittings, including only spin-orbit and electrostatic interactions, are in excellent (0.1%) agreement with the values quoted in Ref. 14 [Eq. (4)] for the 1s₄ and 2s₂ levels. For the 2p₄ level, there is a difference of ~5% in the coefficient of the dominant |³P₂⟩ basis state.

²⁷See for example, B. G. Wybourne, *Spectroscopic Properties of Rare Earths* (Interscience, New York, 1967).

²⁸H. Nagaoka and T. Mishima, *Institute Phys. Chem. Research (Tokyo)* **13**, 293 (1930).

²⁹A. Szöke and A. Javan, *Phys. Rev. Letters* **10**, 521 (1963).

³⁰D. A. Jackson and M. C. Coulombe, *Compt. Rend.* **B268**, 146 (1969).

Atomic *M*-Shell Coster-Kronig, Auger, and Radiative Rates, and Fluorescence Yields for Ca-Th[†]

Eugene J. McGuire

Sandia Laboratories, Albuquerque, New Mexico 87115

(Received 20 October 1971)

Calculated Auger, Coster-Kronig, super Coster-Kronig, and radiative transition rates are used to compute atomic *M*-shell Auger, Coster-Kronig, and fluorescence yields. Comparison is made with five fluorescence-field measurements, with full width at half-maximum measurements of *L-M* x rays, and with Bhalla's relativistic radiative-yield calculations.

I. INTRODUCTION

Little experimental information is available on atomic decay schemes for the *M* shell.¹ Yet such information is useful in interpreting *L-M* x-ray transition half-widths, surface studies based on Auger electron emission, studies of *M*-shell photoabsorption, studies of final charge states following inner-shell ionization, etc. The present author has shown, semiquantitatively, how strongly the lifetime of a *3p* hole affects the photoabsorption cross section in the solids Ti to Co.² In this paper, in addition to comparing calculated and measured mean *M*-shell fluorescence yields, measured and calculated *L-M* x-ray half-widths are compared. In succeeding papers we will examine detailed Auger electron emission spectra following ionization of the *M* shell,³ and study final-charge-state production following ionization of the *K*, *L*, and *M* shell for the elements up to Kr.⁴ However, it must be emphasized that there is little experimental information

available on such gross quantities as fluorescence yields, and none available on Coster-Kronig yields. Thus, the reliability of these results is something of an open question.

II. CALCULATED TRANSITION RATES

Before outlining the procedures used in the calculation we need to supplement the definitions of yields used in the case of *L*-shell decay.¹ The need arises because in the *M* shell for *Z* ≤ 36 there exists the possibility that 3s and 3p holes can decay with the creation of two other *M*-shell holes. These have been called super Coster-Kronig transitions.² Paralleling the definitions used in *L*-shell decay we define ω_{M_i} as the probability that an *M_i*-subshell hole will decay by a radiative transition from a higher shell, but not from a higher *M* subshell (these latter transitions are negligibly weak but are included in the definition of the Coster-Kronig yield). We define a_{M_i} as the probability that an *M_i*-subshell hole

TABLE I. M_1 subshell width and yields. The notation $a E-n$ is $a \times 10^{-n}$.

Z	Γ (eV)	a_{M_1}	ω_{M_1}	$S_{M_1,2}$	$S_{M_1,3}$	$S_{M_1,4}$	$S_{M_1,5}$
20	0.82	0.017	8.4 E-6	0.328	0.655		
22	3.24	0.0040	3.2 E-6	0.319	0.639	0.314	0.471
23	4.18	0.0031	2.9 E-6	0.315	0.631	0.335	0.503
24	4.92	0.0	2.6 E-6	0.319	0.638	0.397	0.596
25	5.92	0.0019	3.1 E-6	0.312	0.623	0.357	0.538
26	6.90	0.0016	2.8 E-6	0.311	0.621	0.371	0.556
27	7.28	0.0013	2.8 E-6	0.308	0.616	0.376	0.564
28	7.92	0.0011	3.5 E-6	0.307	0.614	0.381	0.566
29	6.66	0.0	4.1 E-6	0.304	0.608	0.406	0.610
30	5.90	0.0016	4.6 E-6	0.283	0.566	0.374	0.561
32	4.59	0.0053	9.1 E-6	0.249	0.522	0.273	0.409
36	6.11	0.015	4.9 E-5	0.270	0.540	0.086	0.127
40	6.47	0.027	7.0 E-5	0.278	0.475	0.108	0.163
44	7.89	0.033	1.2 E-4	0.305	0.457	0.065	0.124
47	9.62	0.036	1.7 E-4	0.343	0.461	0.065	0.097
50	10.85	0.045	2.5 E-4	0.315	0.475	0.067	0.101
54	10.18	0.055	4.7 E-4	0.238	0.505	0.081	0.122
57	9.30	0.065	8.4 E-4	0.195	0.506	0.094	0.140
60	12.87	0.053	8.1 E-4	0.236	0.489	0.092	0.128
63	14.95	0.055	8.7 E-4	0.338	0.485	0.070	0.100
67	18.3	0.056	1.08 E-3	0.266	0.527	0.061	0.090
70	20.8	0.053	1.15 E-3	0.272	0.525	0.056	0.091
73	19.3	0.060	1.45 E-3	0.197	0.561	0.065	0.115
76	20.4	0.067	1.65 E-3	0.161	0.594	0.067	0.109
79	20.9	0.074	2.13 E-3	0.148	0.594	0.067	0.112
83	21.7	0.079	2.89 E-3	0.109	0.650	0.065	0.095
86	20.2	0.090	3.95 E-3	0.143	0.593	0.069	0.100
90	22.7	0.080	4.53 E-3	0.072	0.690	0.063	0.091

TABLE II. $4p-3s$ transition rates in 10^{-4} /a.u. (1 a.u. = 2.47×10^{-17} sec). The values of Ref. 11 are taken as the standard in determining the percent difference.

Z	Present calculation	Ref. 11	% Diff.
48	0.69	0.52	33
55	1.80	1.46	23
64	4.55	3.73	22
70	7.50	6.05	24
80	14.4	12.6	14
93	33.5	27.8	21

will decay by a radiationless transition not involving any other M subshell. We slightly modify the definition of the Coster-Kronig yield using f_{M_i} as the probability that an M_i -subshell hole will decay by a process leading to *at least* one other M -subshell hole. Clearly $f_{M_i} = 1 - a_{M_i} - \omega_{M_i}$. We introduce the quantity $S_{M_{ij}}$ defined as the average number of M_j holes occurring in the first step in the decay of an M_i hole. When super Coster-Kronig processes are energetically forbidden $f_{M_i} = \sum_j S_{M_{ij}}$ and the $S_{M_{ij}}$ are similar to the quantities f_{ij} used in discussing the L shell. We emphasize the first step as we have examined the first step only. For instance, it is possible that an M_1 hole can decay by an $M_1-M_2M_{4,5}$

TABLE III. M_2 and M_3 subshell width and yields. The notation $a E-n$ is $a \times 10^{-n}$.

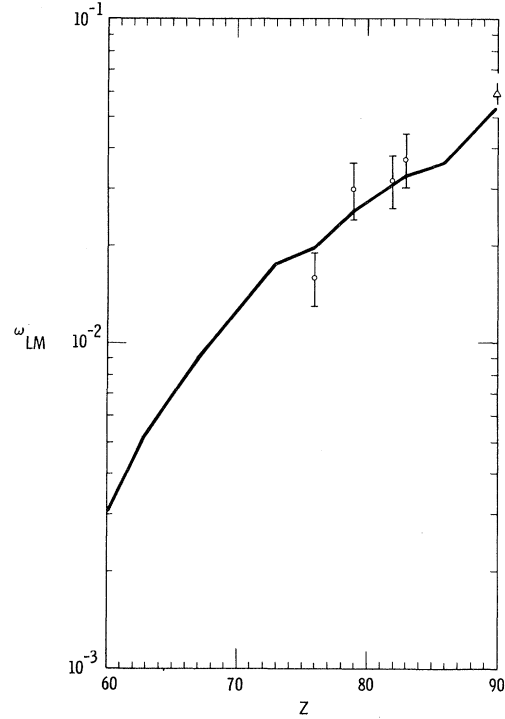
Z	Γ_{M_2} (eV)	a_{M_2}	ω_{M_2}	$S_{M_2,3}$	$S_{M_2,4}$	$S_{M_2,5}$	Γ_{M_3} (eV)	a_{M_3}	ω_{M_3}	$S_{M_3,4}$	$S_{M_3,5}$
20	0.0003	0.938	0.062								
22	0.21	0.0014	3.4 E-5		1.057	0.672				0.509	1.220
23	0.53	0.00066	2.3 E-5		1.089	0.820				0.558	1.280
24	1.32	0.0	1.6 E-5		1.123	0.834				0.612	1.342
25	1.52	0.00017	1.6 E-5		1.108	0.797				0.589	1.317
26	2.15	0.00014	1.6 E-5		1.116	0.815				0.600	1.329
27	2.85	0.00012	1.7 E-5		1.120	0.817				0.602	1.335
28	3.80	0.00005	1.5 E-5		1.122	0.827				0.609	1.341
29	5.22	0.0	1.6 E-5		1.133	0.850				0.623	1.360
30	4.70	0.00009	2.2 E-5		1.107	0.811				0.597	1.320
32	5.22	0.0017	2.6 E-5		1.085	0.786				0.580	1.292
36	4.14	0.015	6.0 E-5		0.919	0.516	4.13	0.015	6.0 E-5	0.395	1.039
40	2.43	0.069	1.4 E-4	0.032	0.591	0.309	2.40	0.070	1.5 E-4	0.252	0.677
44	2.91	0.099	2.6 E-4	0.067	0.550	0.283	2.98	0.091	2.3 E-4	0.236	0.672
47	3.74	0.098	3.9 E-4	0.073	0.570	0.258	3.88	0.089	3.2 E-4	0.223	0.689
50	3.69	0.126	7.0 E-4	0.016	0.604	0.252	4.06	0.107	5.4 E-4	0.213	0.678
54	4.83	0.128	9.0 E-4	0.031	0.612	0.233	5.48	0.106	6.8 E-4	0.206	0.688
57	5.76	0.127	1.10 E-3	0.034	0.557	0.282	5.41	0.125	9.9 E-4	0.198	0.678
60	6.69	0.127	1.32 E-3	0.057	0.644	0.172	6.81	0.113	1.05 E-3	0.174	0.712
63	8.37	0.117	1.47 E-3	0.062	0.514	0.137	7.81	0.114	1.26 E-3	0.165	0.720
67	10.4	0.106	1.85 E-3	0.106	0.667	0.120	10.2	0.103	1.45 E-3	0.145	0.751
70	11.8	0.096	1.97 E-3	0.116	0.680	0.105	11.6	0.095	1.66 E-3	0.141	0.761
73	12.0	0.104	2.64 E-3	0.114	0.674	0.106	10.8	0.104	2.14 E-3	0.082	0.810
76	13.9	0.110	3.25 E-3	0.107	0.684	0.098	9.34	0.126	3.20 E-3	0.106	0.764
79	14.7	0.114	4.23 E-3	0.114	0.673	0.095	9.35	0.158	4.20 E-3	0.114	0.782
83	14.6	0.135	6.52 E-3	0.103	0.662	0.083	10.7	0.155	5.33 E-3	0.094	0.750
86	13.9	0.157	9.75 E-3	0.128	0.610	0.093	11.9	0.152	6.30 E-3	0.072	0.768
90	15.5	0.159	1.40 E-2	0.116	0.623	0.088	12.9	0.170	8.10 E-3	0.097	0.725

TABLE IV. M_2 , M_3 and summed radiative transition rates in $10^{-4}/\text{a.u.}$ (1 a.u. = 2.42×10^{-17} sec).

Z	Present calculations			Ref. 11		Tot
	M_2	M_3	Tot	M_2	M_3	
48	0.66	0.56	1.22	0.60	0.57	1.17
55	1.81	1.55	3.36	1.80	1.79	3.59
64	5.15	4.00	9.15	5.01	4.96	9.97
70	8.55	7.10	15.65	7.93	8.25	16.2
80	25.0	16.2	41.2	19.2	20.5	39.7

transition. It is possible that the M_2 hole in the doubly ionized M shell can then decay by an M_2 - $M_{4,5}$ transition, but this possibility must be determined with the energetics of the doubly ionized M shell, and this we have not examined.

The procedures used in the computations are similar to those in earlier work.⁵ However, because of the dominance of Coster-Kronig and super Coster-Kronig transitions, the calculations were done in j - j coupling. Tables of the j - j coupling transition rates for d holes and f electrons are published elsewhere.⁶ The transition rates and yields do depend on the use of j - j coupling since for the Coster-Kronig and super Coster-Kronig rates we use a continuum electron energy determined from the ESCA tables.⁷ That is, the continuum electron energy is different in an M_1 - M_2M_4 transition than in an M_1 - M_3M_4 transition. The intensities are not necessarily in the ratio 1 to 2. As we did earlier, we determined the one-electron orbitals by approximating the central potential of Herman and Skillman⁸ for an ion with a $3p$ hole by a series of seven straight lines.⁹ The bound and continuum orbitals

FIG. 1. Mean M -shell fluorescence yield ω_{LM} vs Z . The points are from Refs. 12 and 13.

are then obtained in terms of Whittaker functions. The one-electron eigenvalues obtained in the above approximation differ from those of Herman and Skillman. For the Auger and radiative transitions, the model eigenvalues are used in forming energy differences. These are raw calculations which we plot as a function of the most significant model en-

TABLE V. M_4 and M_5 subshell width and yields. The notation $a E-n$ is $a \times 10^{-n}$.

Z	$\Gamma_{M4}(\text{eV})$	a_{M4}	ω_{M4}	$f_{4,5}$	Γ_{M5}	a_{M5}	ω_{M5}	$\omega_{L,M}$
32	0.048	0.997	$2.7 E-3$					
36	0.089	0.997	$2.7 E-3$					
40	0.073	0.997	$2.7 E-3$					
44	0.24	0.997	$2.9 E-3$					
47	0.44	0.997	$2.7 E-3$					
50	0.52	0.997	$2.7 E-3$					
54	0.68	0.997	$2.7 E-3$					
57	0.73	0.997	$2.7 E-3$					
60	1.39	0.722	$2.6 E-3$	0.267	1.00	0.997	$3.2 E-3$	0.0030
63	1.86	0.627	$4.1 E-3$	0.369	1.14	0.994	$5.9 E-3$	0.0052
67	2.41	0.585	$6.7 E-3$	0.408	1.38	0.989	0.0106	0.0090
70	3.10	0.558	$8.6 E-3$	0.479	1.56	0.985	0.0149	0.0124
73	3.25	0.575	0.0130	0.411	1.80	0.979	0.0205	0.0175
76	4.18	0.567	0.0137	0.418	2.25	0.977	0.0232	0.0194
79	2.80	0.928	0.0264	0.046	2.66	0.974	0.0256	0.0259
83	2.88	0.932	0.0330	0.035	2.74	0.967	0.0325	0.0327
86	3.04	0.900	0.0355	0.065	2.81	0.964	0.0362	0.0359
90	3.22	0.874	0.0582	0.066	2.92	0.950	0.0497	0.0531

than 20%.

VI. FULL WIDTH AT HALF-MAXIMUM FOR SOME L-M X-RAY LINES

The full width at half-maximum of an x-ray emission line measures the sum of widths due to the two levels involved in the transition, i. e., $\Gamma_{PQ} = \Gamma_P + \Gamma_Q$. This has proved useful in the analysis of K hole total transition rates since $\Gamma_K \gg \Gamma_L$ and the width of a K-L emission line is a measure of Γ_K . One cannot use the measured width of L-M emission lines to determine Γ_L because $\Gamma_L \sim \Gamma_M$. However, with both Γ_L and Γ_M calculated, we can compare the calculated width, $\Gamma_L + \Gamma_M$, with measurements. This is done in Table VII. The calculations are compared with the measurements of Parratt on Ag,¹⁴ of Williams on W, Au, and Bi,¹⁵ and of Williams on U.¹⁶ The measurements for U are compared with the calculations for Z=90. For transitions to 2p holes the calculations are in reasonable agreement with experiment, while for transitions to 2s holes there is severe disagreement. Crasemann *et al.*¹⁷ have computed L₁ shell widths using screened hydrogenic wave functions and find $\Gamma_{L1} = 7.56$ eV for Ag, while we have $\Gamma_{L1} = 9.03$ eV. This leads to values of $\Gamma_{L1} + \Gamma_M$ closer to the measured values than ours, but still their results are significantly different from experiment. There is a striking difference between our calculated β_3 width for Z=90 and Williams's measurements on U. Yet for the β_4 width,

calculation and experiment are in excellent agreement.

VII. DISCUSSION

We have presented transition rates and yields for the decay of M-subshell holes. Fluorescence yields for the M₄ and M₅ subshells were compared with measurements on five elements. Four of the measurements were accurate to 20% and the error bars overlap the calculations in three of the four cases. At Z=76, the calculation and experiment agree to 25%. Comparison was made with x-ray full widths at half-maximum. For L₂M₄ and L₃M₄, M₅ transitions, calculation and experiment agree to 20%. However, for the L₁M₂, M₃ x-ray full widths at half-maximum there are significant differences. Interpolated radiative yields were compared with Bhalla's relativistic Hartree-Fock-Slater calculations with agreement, in general, to 25%. Again, we emphasize that while we have extensive yield calculations for the M shell and while the calculations are in reasonable agreement with measurements, the paucity of experimental data precludes one from estimating the reliability of the calculations to better than 25%.

ACKNOWLEDGMENT

I wish to thank Professor Crasemann for informing me of his group's work prior to publication.

†Work supported by the U. S. Atomic Energy Commission.

¹R. W. Fink, R. C. Jopson, H. Mark, and C. D. Swift, *Rev. Mod. Phys.* **38**, 513 (1966).

²E. J. McGuire, *J. Phys. Chem. Solids* (to be published).

³E. J. McGuire, second following paper, *Phys. Rev. A* **5**, xxx (1972).

⁴E. J. McGuire, *Phys. Rev. A* (to be published).

⁵E. J. McGuire, *Phys. Rev. A* **3**, 587 (1971).

⁶E. J. McGuire, *Nucl. Phys. A* **172**, 127 (1971).

⁷K. Siegbahn *et al.*, in *ESCA, Atomic, Molecular and Solid State Structure Studied by Means of Electron Spectroscopy* (Nova Acta Regiae Societatis Upsaliensis, Uppsala, 1967), Ser. IV, Vol. 20.

⁸F. Herman and S. Skillman, *Atomic Structure Calculations* (Prentice-Hall, Englewood Cliffs, N. J., 1963).

⁹A complete set of matrix elements and transition rates in *j-j* coupling are available from the author. E. J. McGuire, Sandia Laboratories Research Report No. SC-RR-710835 (unpublished).

¹⁰Energy differences obtained from the ESCA tables are taken as "true" in the absence of complete tables of M-shell x-ray energies.

¹¹C. P. Bhalla, *J. Phys. B* **3**, 916 (1970).

¹²R. C. Jopson, H. Mark, C. D. Swift, and M. A. Williamson, *Phys. Rev.* **137**, A1353 (1965).

¹³H. Lay, *Z. Physik* **91**, 533 (1934).

¹⁴L. G. Parratt, *Phys. Rev.* **54**, 99 (1938).

¹⁵J. H. Williams, *Phys. Rev.* **45**, 71 (1934).

¹⁶J. H. Williams, *Phys. Rev.* **37**, 1431 (1931).

¹⁷B. Crasemann, M. H. Chen, and V. O. Kostroun, *Phys. Rev. A* **4**, 2161 (1971).